New data on activation cross section for deuteron induced reactions on ytterbium up to 50 MeV

F. Tárkányi[a], F. Ditrói[a,*], S. Takács[a], A. Hermanne[b], A.V. Ignatyuk[c]

[a] *Institute for Nuclear Research, Hungarian Academy of Sciences (ATOMKI), Debrecen, Hungary*
[b] *Cyclotron Laboratory, Vrije Universiteit Brussel (VUB), Brussels, Belgium*
[c] *Institute of Physics and Power Engineering (IPPE), Obninsk, Russia*

arXiv:1412.0853v1 [nucl-ex] 2 Dec 2014

Abstract

Activation cross sections of deuteron induced reactions on ytterbium for production of ^{177g,173,172,171,170,169,167}Lu, ^{177,175,169}Yb and ^{173,168,167,165}Tm were extended up to 50 MeV deuteron energy. The new data are in acceptable agreement with the earlier experimental data in the overlapping energy region. The experimental data are compared with the predictions of the ALICE-D, EMPIRE-D and TALYS 1.4 (TENDL-2013 on-line library results) codes.

Keywords: ytterbium target, deuteron activation, Lu, Yb and Tm radioisotopes

1. Introduction

To meet the requirements of improving the reliability of available experimental and theoretical cross section data, we started to establish an experimental database some years ago, by performing new experiments and making a systematical survey of published deuteron induced activation cross-sections up to 50 MeV [1]. In an earlier publication we presented the activation cross-sections of longer-lived products of deuteron induced nuclear reactions on ytterbium up to 40 MeV, obtained in irradiations at the Sendai cyclotron [2]. The earlier data of Nichols et al. [3], Hermanne et al., [4], Manenti et al. [5] and Dmitriev et al. [6] were discussed in more detail at energies below 30 MeV in this publication. Since that time only one new work was published by Manenti et al. on physical optimization of production of high specic activity ^{177g}Lu by deuteron irradiation [7]. We have had now the possibility to extend the energy range up to 50 MeV deuteron energy and to investigate some shorter-lived reaction products (in the 40 MeV experiments the first γ-spectra could only be measured one day after end of bombardment). To avoid repetition of the content of our previous paper [2] we describe the experiment, the results and the theoretical comparisons only in summary form.

2. Experiment and data evaluation

For measurements, the well-known stacked foil irradiation technique and high resolution γ-spectrometry were used. Yb metal foils, interleaved with Al foils for monitoring beam characteristics were stacked and irradiated at the UCL (LLN) cyclotron. The Yb foils were irradiated together with Nd foils. The report on activation cross section data on Nd is in progress [8]. The main experimental parameters and methods of data evaluation are summarized in Table 1. The complete excitation function was measured for the ^{nat}Al(d,x)^{24}Na monitor reactions, allowing to control the beam intensity and the energy by comparison with recommended data [9], and are shown in Fig. 1 in our earlier submitted paper on nuclear reactions on simultaneously irradiated Nd [7]. The decay characteristics of the investigated reaction products and the possibly contributing reactions in the energy region studied are summarized in Table 2. It should be mentioned that in a few cases we could not find independent γ-lines to assess the produced activity of the investigated radioisotopes. In these cases the contributions of the overlapping γ-lines from the decay of the other nuclides were subtracted.

3. Comparison with the results of model codes

In our previous work we made calculations for the investigated reactions using the modified model codes ALICE-IPPE [17] and EMPIRE-II [18]. In the used

*Corresponding author: ditroi@atomki.hu

Table 1: Main experimental parameters and main parameters and methods of the data evaluation

Main experimental parameters		**Methods of the data evaluation**	
Incident particle	Deuteron (LLN)	Gamma spectra evaluation	Genie 2000[10], Forgamma [11]
Method	Stacked foil	Determination of beam intensity	Faraday cup (preliminary) Fitted monitor reaction (final) [12]
Target composition	^{nat}Nd (100 μm)-target ^{nat}Yb(22.88 μm)-target Al (49.06 μm)-monitor (repeated 19 times) Interleaved with Al (156.6 μm, 103.43 μm, 49.06 μm)-energy degraders	Determination of beam intensity	Faraday cup (preliminary) Fitted monitor reaction (final)[9, 12]
Number of Yb target foils	19	Decay data (see Table 2)	NUDAT 2.6 [13]
Accelerator	Cyclone110 cyclotron of Universit Catholique in Louvain la Neuve (LLN) Belgium	Reaction Q-values(see Table 2)	Q-value calculator [14]
Primary energy	50 MeV	Determination of beam energy	Andersen (preliminary[15] Fitted monitor reaction (final) [9]
Covered energy range	48.2-12.9 MeV	Uncertainty of energy	Cumulative effects of possible uncertainties (primary energy, target thickness, energy straggling, correction to monitor reaction)
Irradiation time	60 min	Cross sections	Isotopic and elemental cross sections
Beam current	92 nA	Uncertainty of cross sections	Sum in quadrature of all individual contributions: beam current (7%), beam-loss corrections (max. of 1.5%), target thickness (1%), detector efficiency (5%), photo peak area determination and counting statistics (1-20 [16]
Monitor reaction [recommended values]	^{27}Al(d,x)^{24}Na reaction [9] (re-measured over the whole energy range)		
Monitor target and thickness	*Cityplacenat* Al, 49.06 mm		
detector	HPGe		
Chemical separation	no		
γ-spectra measurements	3 series		
Cooling times (and corresponding target-detector distances)	2.1-5.5 h (25 cm) 23.7-30.7 h (15 cm) 36.9-432.2 h (5cm)		

modified code versions ALICE-IPPE-D and EMPIRE-D, the direct (d,p) channel is increased strongly [19, 20]. Here we repeat these results for comparison above 40 MeV too. The new experimental data are also compared with the cross section data reported in the TALYS 1.4 based [21] TENDL-2013 data libraries [22].

4. Results

The cross-sections for all reactions investigated are shown in Figs. 114 and the numerical values are shown in Tables 3-4. The contributing reactions can be found in Table 2. The reactions were discussed in detail in our previous work [2]. The agreement (or disagreement) of the new data with the previous experimental data and with the model results are shown in the corresponding figures and discussed below. The new results are in acceptable agreement with the previous data in most cases. As in [2] we deduced already integral yields for production of the investigated reaction products up to 40 MeV, we did not include in this paper a new figure extended to 50 MeV.

4.1. ^{177g}*Lu (cum)*

The cumulative production of ^{177g}Lu (6.71 d half-life) following the total decay of parent ^{177}Yb ($T_{1/2}$ = 1.9 h) was detected. It practically contains no contribution from the internal decay of ^{177m}Lu (160.4 d, IT 21.7%) (long-lived, low formation cross-section). Only two cross section points were reliably assessed, near the maximum (Fig. 1). The new data are in good agreement with our earlier results, but somewhat higher than the results of Manenti [5] and Hermanne [4]. The nuclear model codes, especially the TENDL-2013 give lower values in this energy region.

4.2. ^{173}*Lu*

The production of ^{173}Lu (1.37 a) arises from ^{nat}Yb(d,xn)^{173}Lu reactions on different stable Yb isotopes (Fig. 2). The new data are in good agreement with our earlier results [2] and also with those of Manenti [5] and Hermanne [4]. The values of Nichols [3] do not even reproduce the first maximum. The nuclear model codes follow the shape of the experimental curve and also the values, but it is difficult to judge, which of them gives the best approximation.

4.3. ^{172g}*Lu (m+)*

The cross sections contain the complete contribution of the decay of short-lived isomeric state (3.7 min) (Fig. 3). Our new data are in good agreement with the earlier experimental results. The best approximation is given by the TALYS (TENDL-2013) nuclear reaction model

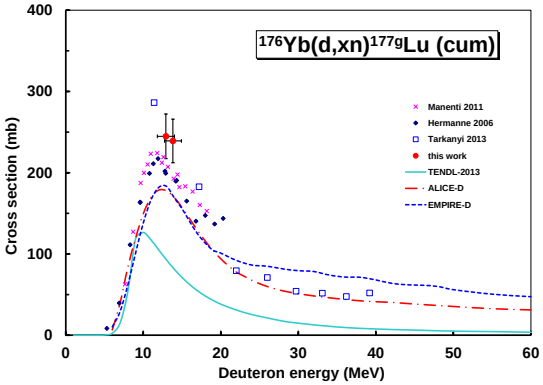

Figure 1: Excitation function of the ^{176}Yb(d,x)^{177g}Lu reaction

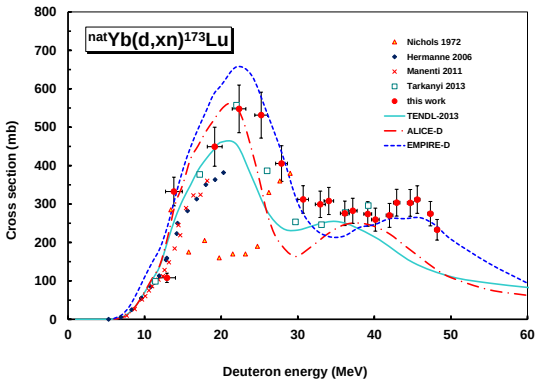

Figure 2: Excitation function of the ^{nat}Yb(d,xn)^{173}Lu reaction

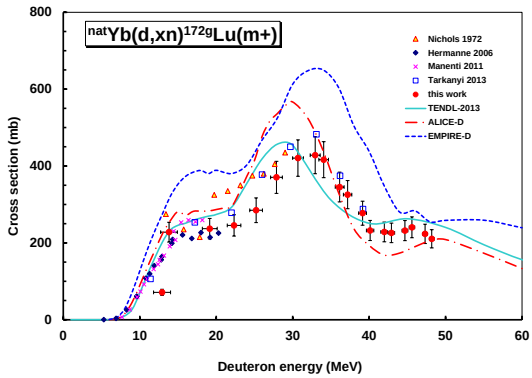

Figure 3: Excitation function of the ^{nat}Yb(d,xn)^{172mg}Lu reaction

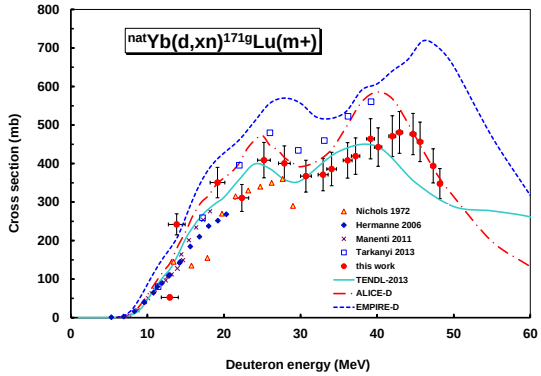

Figure 4: Excitation function of the ^{nat}Yb(d,xn)^{171mg}Lu reaction

code, while both other codes overestimate the maximum and also the maximum energy.

4.4. ^{171g}Lu (m+)

The cumulative production of 171Lu (8.24 d) includes the complete decay through isomeric transition of the short-lived (79 s) isomeric state (Fig. 4). The new data are in good agreement with our former results, with the experimental results of Hermanne [4] and Manenti [5], but give somewhat lower values than our previous results between 20 and 40 MeV. The best estimate is given by the TENDL-2013 prediction.

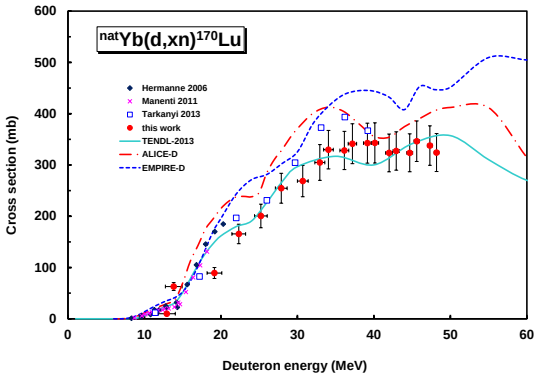

Figure 5: Excitation function of the ^{nat}Yb(d,xn)^{170}Lu reaction

4.5. ^{170}Lu

No parent contribution exists for the formation of ^{170}Lu (no isomeric state), so the presented results are direct cross-sections resulting from (d,xn) reactions (Fig. 5). Our new data are in good agreement with the previous experimental results, except the first local maximum, where our previous results were slightly higher. The best computational approximation is given by the TENDL-2013 library again.

4.6. ^{169}Lu

^{169}Lu (32.018 d) is produced directly via the ^{nat}Yb(d,xn) reactions (Fig. 6). The new data are in good agreement with our previous experimental results. The best model approach is given by the TENDL-2013 library again.

4.7. ^{167}Lu

No earlier experimental data were found for the formation of ^{167}Lu through the ^{nat}Yb(d,xn)^{167}Lu reactions. Our new data for production of ^{167}Lu (51.5 min) are presented in Fig. 7. Our new experimental data are below all predictions of the nuclear reaction model codes.

4.8. ^{177}Yb

In our previous measurement up to 40 MeV [2] we could not identify the γ-lines of ^{177}Yb (1.911 h) in our spectra due to the long cooling time. As in these experiments measurements could be started 2 h after EOB, a statistically significant signal for the independent 150.3 keV line of ^{177}Yb could be identified. The new results are shown in Fig. 8, and are in good agreement

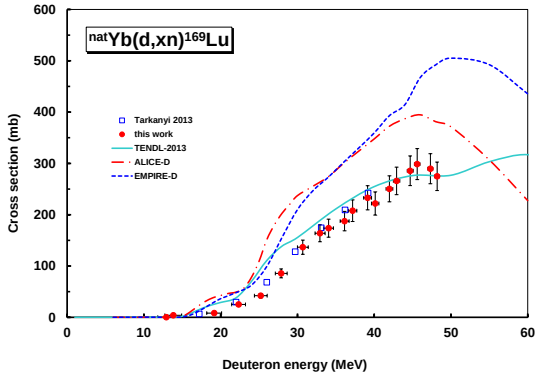

Figure 6: Excitation function of the ^{nat}Yb(d,xn)^{169}Lu reaction

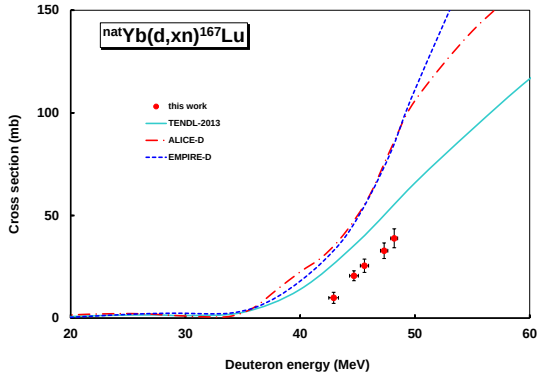

Figure 7: Excitation function of the ^{nat}Yb(d,xn)^{167}Lu reaction

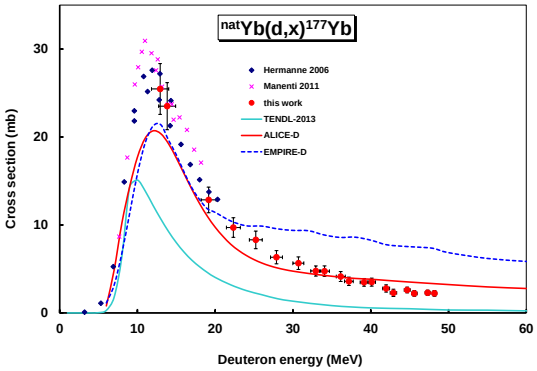

Figure 8: Excitation function of the ^{176}Yb(d,p)^{177}Yb reaction

with [4] and [5]. ^{177}Yb can only be produced via the ^{176}Yb(d,p)^{177}Yb reaction. All nuclear reaction model codes underestimate the maximum value, the best estimate is given by the ALICE-D code (due to its improved (d,p) capability).

4.9. ^{175}Yb (cum)

The cumulative production of ^{175}Yb (4.185 d) (via direct (d,pxn) reactions and from β^--decay of ^{175}Tm (15.2 min)) is shown in Fig. 9. Our new data support the earlier data from our group [2, 5] in the lower energy region due to the ^{176}Yb(d,2pn) reaction. All nuclear reaction codes underestimate the experimental values, only the first maximum energy is given correctly by the ALICE-D and EMPIRE-D codes. The second broad maximum is only predicted by the TENDL-2013 library.

4.10. ^{169}Yb (cum)

The measured cumulative activation cross-sections of ^{169}Yb ($T_{1/2}$ = 32.018 d) are shown in Fig. 10. This radioisotope is obtained through direct production via ^{nat}Yb(d,pxn) reactions and from the decay of the shorter-lived parent ^{169}Lu (34.06 h). Our new data are in good agreement with our previous results in the overlapping energy range and also with the other experiment in the low energy region. Now, all the nuclear reaction model codes give similar results in the measured energy region. The TENDL-2013 prediction seems to be the closest approximation, but it does not predict the expected maximum below 50 MeV.

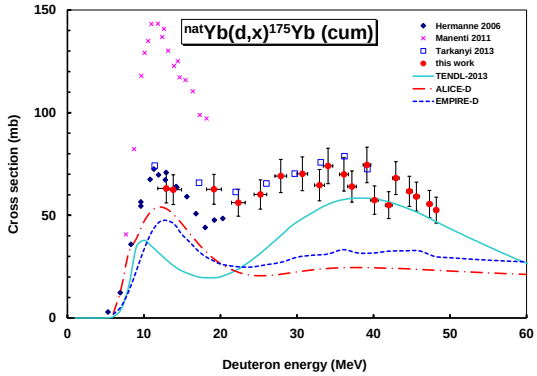

Figure 9: Excitation function of the ^{nat}Yb(d,x)^{175}Yb process

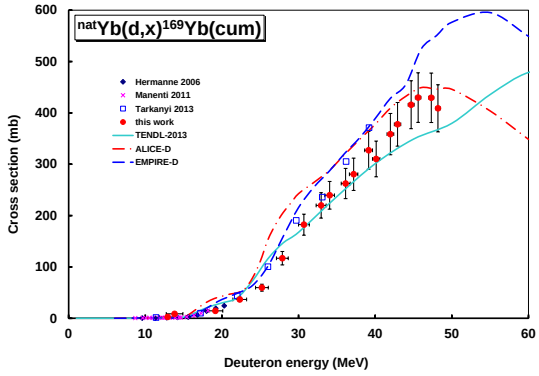

Figure 10: Excitation function of the ^{nat}Yb(d,x)^{169}Yb reaction

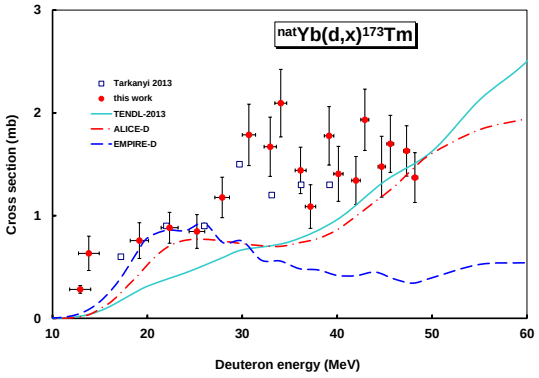

Figure 11: Excitation function of the ^{nat}Yb(d,x)^{173}Tm reaction

4.11. ^{173}Tm

The cross sections of directly produced ^{173}Tm (8.24 h) are presented on Fig. 11. In spite of the quite strong scattering, our new experimental data support our previous measurement. EMPIRE-D and ALICE-D give acceptable estimates below 27 MeV, reproducing the first local maximum too, while TALYS completely fails in this case.

4.12. ^{168}Tm

The measured excitation function for direct production of ^{168}Tm (93.1 d) is shown in Fig. 12. Because of the low statistics the data are scattered again, but the good agreement with our previous results is obvious. All nuclear reaction model codes, especially TALYS, underestimate the experimental values.

4.13. ^{167}Tm (cum)

The excitation function for cumulative production of ^{167}Tm (9.25 d) (direct reactions and from the decay of short-lived parent ^{167}Yb (17.5 min)) are sown in Fig. 13. The best prediction is provided by the TENDL-2013 library above 35 MeV, while under 35 MeV all the three codes show approximately the same results.

4.14. ^{165}Tm (cum)

The measured excitation function for ^{165}Tm (30.06 h) is shown in Fig. 14. It was produced both directly through ^{nat}Yb(d,pxn) reactions and indirectly from decay of short-lived parent ^{165}Yb (9.9 min). The overlap with our previous results is acceptable. The best prediction is given by the ALICE-D code in this case.

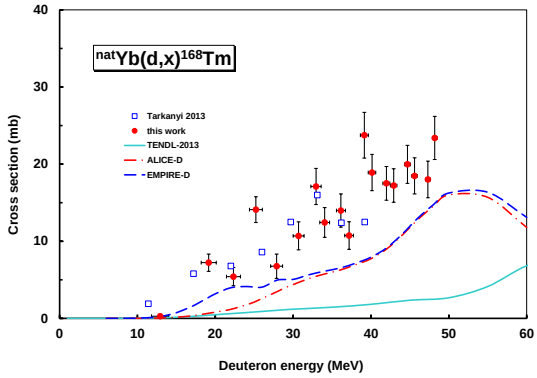

Figure 12: Excitation function of the ^{nat}Yb(d,x)^{168}Tm reaction

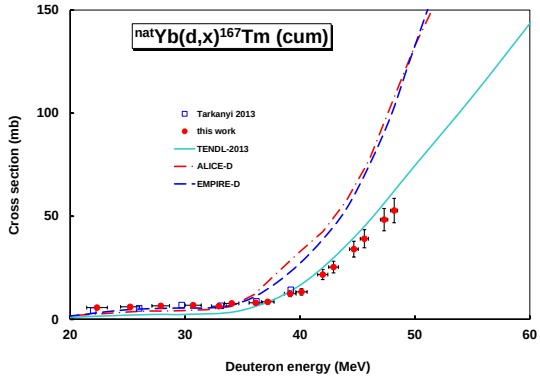

Figure 13: Excitation function of the ^{nat}Yb(d,x)^{167}Tm reaction

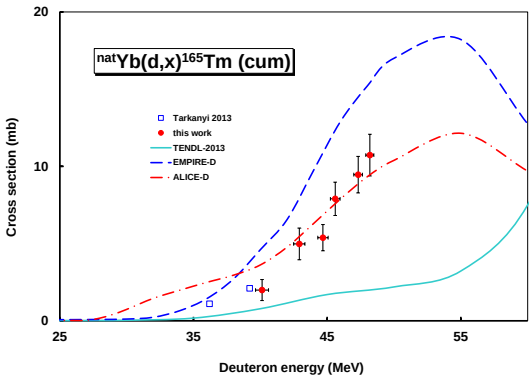

Figure 14: Excitation function of the ^{nat}Yb(d,x)^{165}Tm reaction

5. Summary and conclusion

Excitation functions of deuteron induced nuclear reactions on natural Yb were measured up to 50 MeV, as an extension and improvement of our earlier works. The comparison with the earlier experimental data, measured at lower energies, shows acceptable agreement (except for ^{173}Lu and ^{175}Yb). The experimental data were compared with the results of our ALICE-D and EMPIRE-D calculations and with the data in the TENDL-2013 library based on TALYS 1.4 calculations. The theoretical descriptions of the experimental excitation functions in shape and in absolute values are acceptable if we consider the large disagreements of the earlier versions of the used model codes. The obtained experimental data provide a basis for improved model calculations and for applications in different fields of nuclear medicine (e.g. cancer treatment), as tracer in nuclear biology, in industry and for non-destructive testing and as radioactive tracers in different processes (for related references see our earlier work [2]).

6. Acknowledgements

This work was performed in the frame of the HAS-FWO Vlaanderen (Hungary-Belgium) project. The authors acknowledge the support of the research project and of the respective institutions in providing the beam time and experimental facilities.

Correction

During the EXFOR compilation of our previous paper on cross sections for deuteron induced processes on Yb (F. Tarkanyi et al., Nucl. Instrum. Meth. section B, 304(2013)36-48 [2]) it was discovered that the decay data of ^{169}Lu are misprinted in Table 1 of that publication. However, the cross section values presented in the tables and in the figures are correct. The ^{169}Yb decay data used in the calculations are: $T_{1/2}$-34.04 h, $E_\gamma(I_\gamma)$-191.214 keV (20.6 %) and 960.622 keV (23.4 %).

References

[1] F. Tárkányi, A. Hermanne, F. Ditrói, S. Takács, B. Király, G. Csikai, M. Baba, H. Yamazaki, M. S. Uddin, A. V. Ignatyuk, S. M. Qaim, Systematic study of activation cross-sections of deuteron induced reactions used in accelerator applications (25-28 Oct., 2010 2011).

[2] F. Tárkányi, F. Ditrói, S. Takács, A. Hermanne, H. Yamazaki, M. Baba, A. Mohammadi, A. V. Ignatyuk, Activation cross-sections of longer lived products of deuteron induced nuclear reactions on ytterbium up to 40 mev, Nuclear Instruments and Methods in Physics Research B 304 (2013) 36–48.

[3] A. L. Nichols, R. J. Bullock, P. Glentworth, N. R. Large, Excitation functions for the formation of various gadolinium and lutetium isotopes by (d,xn) reactions, Tech. rep., Atomic Energy Research Establishment, Harwell (England) (1972).

[4] A. Hermanne, S. Takacs, M. B. Goldberg, E. Lavie, Y. N. Shubin, S. Kovalev, Deuteron-induced reactions on yb: Measured cross sections and rationale for production pathways of carrier-free, medically relevant radionuclides, Nuclear Instruments and Methods in Physics Research Section B: Beam Interactions with Materials and Atoms 247 (2) (2006) 223–231.

[5] S. Manenti, F. Groppi, A. Gandini, L. Gini, K. Abbas, U. Holzwarth, F. Simonelli, M. Bonardi, Excitation function for deuteron induced nuclear reactions on natural ytterbium for production of high specific activity lu-177g in no-carrier-added form for metabolic radiotherapy, Applied Radiation and Isotopes 69 (1) (2011) 37–45.

[6] P. P. Dmitriev, N. N. Krasnov, G. A. Molin, Radioactive nuclide yields for thick target at 22 mev deuterons energy, Yadernie Konstanti 34 (4) (1982) 38.

[7] S. Manenti, M. L. Bonardi, L. Gini, F. Groppi, Physical optimization of production by deuteron irradiation of high specific activity 177glu suitable for radioimmunotherapy, Nuclear Medicine and Biology in print (0).

[8] F. Tárkányi, S. Takács, F. Ditrói, A. Hermanne, H. Yamazaki, M. Baba, A. Mohammadi, A. V. Ignatyuk, Activation cross-sections of deuteron induced nuclear reactions on neodymium up to 50 mev, Nuclear Instruments and Methods in Physics Research Section B: Beam Interactions with Materials and Atoms 325 (0) (2014) 15–26.

[9] F. Tárkányi, S. Takács, K. Gul, A. Hermanne, M. G. Mustafa, M. Nortier, P. Oblozinsky, S. M. Qaim, B. Scholten, Y. N. Shubin, Z. Youxiang, Beam monitor reactions (chapter 4). charged particle cross-section database for medical radioisotope production: diagnostic radioisotopes and monitor reactions., Tech. rep., IAEA (2001).

[10] Canberra, http://www.canberra.com/products/radiochemistry_lab-/genie-2000-software.asp. (2000).

[11] G. Székely, Fgm - a flexible gamma-spectrum analysis program for a small computer, Computer Physics Communications 34 (3) (1985) 313–324.

[12] F. Tárkányi, F. Szelecsényi, S. Takács, Determination of effective bombarding energies and fluxes using improved stacked-foil technique, Acta Radiologica, Supplementum 376 (1991) 72.

[13] NuDat, Nudat2 database (2.6) http://www.nndc.bnl.gov/nudat2/ (2014).
[14] B. Pritychenko, A. Sonzogni, Q-value calculator, http://www.nndc.bnl.gov/qcalc (2003).
[15] H. H. Andersen, J. F. Ziegler, Hydrogen stopping powers and ranges in all elements. The stopping and ranges of ions in matter, Volume 3., The Stopping and ranges of ions in matter, Pergamon Press, New York, 1977.
[16] I.-B. of-Weights-and Measures, Guide to the expression of uncertainty in measurement, 1st Edition, International Organization for Standardization, Genve, Switzerland, 1993.
[17] A. I. Dityuk, A. Y. Konobeyev, V. P. Lunev, Y. N. Shubin, New version of the advanced computer code alice-ippe, Tech. rep., IAEA (1998).
[18] M. Herman, R. Capote, B. V. Carlson, P. Oblozinsky, M. Sin, A. Trkov, H. Wienke, V. Zerkin, Empire: Nuclear reaction model code system for data evaluation, Nuclear Data Sheets 108 (12) (2007) 2655–2715.
[19] F. Tárkányi, A. Hermanne, S. Takács, F. Ditrói, I. Spahn, S. F. Kovalev, A. V. Ignatyuk, S. M. Qaim, Activation cross sections of the tm-169(d,2n) reaction for production of the therapeutic radionuclide yb-169, Applied Radiation and Isotopes 65 (6) (2007) 663–668.
[20] F. Tárkányi, A. Hermanne, S. Takács, K. Hilgers, S. F. Kovalev, A. V. Ignatyuk, S. M. Qaim, Study of the 192os(d,2n) reaction for, production of the therapeutic radionuclide 192ir in no-carrier added form, Applied Radiation and Isotopes 65 (11) (2007) 1215–1220.
[21] A. J. Koning, S. Hilaire, M. C. Duijvestijn, Talys-1.0 (2007).
[22] A. J. Koning, D. Rochman, S. van der Marck, J. Kopecky, J. C. Sublet, S. Pomp, H. Sjostrand, R. Forrest, E. Bauge, H. Henriksson, O. Cabellos, S. Goriely, J. Leppanen, H. Leeb, A. Plompen, R. Mills, Tendl-2013: Talys-based evaluated nuclear data library (2012).

Table 2: Decay characteristics of the investigated reaction products and the contributing reactions

Nuclide	Half-life	E_γ(keV)	I_γ(%)	Contributing reaction	Q-value (MeV)
^{177g}Lu ε: 100 %	6.647 d	112.9498 208.3662	6.17 10.36	^{176}Yb(d,n) ^{177}Yb decay	3.9
^{173}Lu ε: 100 %	1.37 a	78.63 100.724 272.105	11.9 5.24 21.2	^{172}Yb(d,n) ^{173}Yb(d,2n) ^{174}Yb(d,3n) ^{176}Yb(d,5n)	2.7 -3.7 -11.1 -23.9
^{172g}Lu ε: 100 %	6.70 d	78.7426 181.525 810.064 900.724 912.079 1093.63	10.6 20.6 16.6 29.8 15.3 63	^{171}Yb(d,n) ^{172}Yb(d,2n) ^{173}Yb(d,3n) ^{174}Yb(d,4n) ^{176}Yb(d,6n)	2.5 -5.5 -11.9 -19.4 -32.0
^{171g}Lu ε: 100 %	8.24 d	667.422 739.793 780.711 839.961	11.1 47.9 4.37 3.05	^{170}Yb(d,n) ^{171}Yb(d,2n) ^{172}Yb(d,3n) ^{173}Yb(d,4n) ^{174}Yb(d,5n) ^{176}Yb(d,7n)	2.1 -4.5 -12.5 -18.9 -26.3 -39.0
^{170}Lu ε: 100 %	2.012 d	84.262 193.13 572.20 985.10 1054.28 1138.65 1280.25 1341.20 1364.60	8.7 2.07 1.25 5.4 4.60 3.49 7.9 3.15 4.47	^{170}Yb(d,2n) ^{171}Yb(d,3n) ^{172}Yb(d,4n) ^{173}Yb(d,5n) ^{174}Yb(d,6n) ^{176}Yb(d,8n)	-6.5 -13.1 -21.1 -27.5 -34.9 -47.6
^{169}Lu ε: 100 %	34.06 h	191.217 960.622	18.7 21.2	^{168}Yb(d,n) ^{170}Yb(d,3n) ^{171}Yb(d,4n) ^{172}Yb(d,5n) ^{173}Yb(d,6n) ^{174}Yb(d,7n) ^{176}Yb(d,9n)	1.6 -13.8 -20.4 -28.4 -34.8 -42.2 -54.
^{167}Lu ε: 100 %	51.5 min	178.87 213.20 239.22 401.17 1267.26	2.5 3.33 7.7 3.17 3.87	^{168}Yb(d,3n) ^{170}Yb(d,5n) ^{171}Yb(d,6n) ^{172}Yb(d,7n) ^{173}Yb(d,8n) ^{174}Yb(d,9n) ^{176}Yb(d,11n)	-15.2 -30.5 -37.1 -45.1 -51.5 -59.0
^{177}Yb β^-: 100 %	1.911 h	150.3	20.5	^{176}Yb(d,p)	3.3
^{175}Yb β^-: 100 %	4.185 d	113.805 282.522 396.329	3.87 6.13 13.2	^{174}Yb(d,p) ^{176}Yb(d,p2n) ^{175}Tm decay	3.6 -9.1
^{169}Yb ε: 100 %	32.018 d	109.77924 130.52293 177.21307 197.95675 307.52 307.73586	17.39 11.38 22.28 35.93 0.3 10.05	^{168}Yb(d,p) ^{170}Yb(d,p2n) ^{171}Yb(d,p3n) ^{172}Yb(d,p4n) ^{173}Yb(d,p5n) ^{174}Yb(d,p6n) ^{176}Yb(d,p8n) ^{169}Lu decay	4.6 -10.7 -17.3 -25.3 -31.7 -39.2 -51.9
^{173}Tm β^-: 100 %	8.24 h	398.9 461.4	87.9 6.9	^{173}Yb(d,2p) ^{174}Yb(d,2pn) ^{176}Yb(d,2p3n)	-2.7 -10.2 -22.9
^{172}Tm β^-: 100 %	63.6 h	78.750 181.520 1093.59 1387.093	6.5 2.8 6.0 5.6	^{172}Yb(d,2p) ^{173}Yb(d,2pn) ^{174}Yb(p,2p2n) ^{176}Yb(p,2p4n)	-3.3 -9.7 -17.2 -29.8
^{168}Tm ε: 99.99 % β^-: 0.01 %	93.1 d	79.804 184.295 198.251 447.515 720.392 741.355 815.989 821.162	10.95 18.55 54.49 23.98 12.207 12.81 50.95 11.99	^{168}Yb(d,2p) ^{170}Yb(d,2p2n) ^{171}Yb(d,2p3n) ^{172}Yb(d,2p4n) ^{173}Yb(d,2p5n) ^{174}Yb(d,2p6n) ^{176}Yb(d,2p8n)	-1.7 -17.0 -23.7 -31.7 -38.0 -45.5 -58.2
^{167}Tm ε: 100 %	9.25 d	207.801 531.54	42 1.61	^{168}Yb(d,2pn) ^{170}Yb(d,2p3n) ^{171}Yb(d,2p4n) ^{172}Yb(d,2p5n) ^{173}Yb(d,2p6n) ^{174}Yb(d,2p7n) ^{176}Yb(d,2p9n) ^{167}Yb decay	-8.5 -23.9 -30.5 -38.5 -44.9 -52.3 -65.0
^{165}Tm ε: 100 %	30.06 h	242.917 296.49 297.369 460.263	35.5 3.88 12.7 4.12	^{168}Yb(d,2p3n) ^{170}Yb(d,2p5n) ^{171}Yb(d,2p6n) ^{172}Yb(d,2p7n) ^{173}Yb(d,2p8n) ^{174}Yb(d,2p9n) ^{176}Yb(d,2p11n) ^{165}Yb decay	-24.3 -39.6 -46.2 -54.3 -60.6 -68.1

*When complex particles are emitted instead of individual protons and neutrons the Q-values have to be decreased by the respective binding energies of the compound particles: np-d, +2.2 MeV; 2np-t, +8.48 MeV; 2p2n-a, 28.30 MeV.
**Abundance of isotopes in natural Yb (%): ^{168}Yb-0.13, ^{170}Yb-3.05, ^{171}Yb-14.3, ^{172}Yb-21.9, ^{173}Yb-16.12, ^{174}Yb-31.8, ^{176}Yb-12.7. ***The Q-values refer to formation of the ground state and were obtained from [14]

Table 3: Measured cross-sections of the ^{nat}Yb(d,xn)^{177,173,172mg,171mg,170,169}Lu reactions

Energy E±ΔE (MeV)		Cross section $\sigma \pm \Delta\sigma$ (mb)											
		^{177}Lu		^{173}Lu		^{172g}Lu		^{171g}Lu		^{170}Lu		^{169}Lu	
48.2	0.3			233.1	26.8	210.5	23.8	347.8	39.2	324.2	37.0	274.9	27.8
47.3	0.3			274.9	31.8	223.4	25.2	393.9	44.4	337.8	38.5	289.6	29.3
45.6	0.4			311.6	35.8	240.4	27.1	456.4	51.4	346.3	39.5	298.6	30.2
44.7	0.4			303.0	34.8	231.9	26.2	476.6	53.7	323.6	37.0	285.6	28.9
42.9	0.4			303.7	34.8	226.0	25.5	480.9	54.1	327.2	37.3	265.9	26.9
42.0	0.4			270.6	31.1	228.4	25.8	471.0	53.0	323.4	36.9	250.4	25.3
40.1	0.5			259.6	30.0	232.2	26.2	442.8	49.9	342.9	39.2	221.8	22.4
39.1	0.5			274.2	31.8	277.3	31.2	464.2	52.2	342.6	39.0	232.9	23.6
37.2	0.6			282.5	32.7	325.4	36.7	419.3	47.2	341.3	38.9	207.8	21.0
36.1	0.6			275.9	31.9	345.3	38.9	408.3	46.0	328.2	37.3	187.5	19.0
34.1	0.6			308.0	35.3	416.4	46.9	385.8	43.5	329.7	37.6	173.8	17.6
32.9	0.7			299.4	34.4	428.1	48.2	371.0	41.8	304.8	34.9	163.9	16.6
30.7	0.7			312.0	35.8	420.6	47.3	367.3	41.4	268.6	30.7	136.7	13.8
27.9	0.8			405.4	46.3	370.5	41.7	400.5	45.1	254.6	29.1	85.6	8.7
25.2	0.8			531.5	59.8	284.8	32.1	408.9	46.1	200.5	23.1	42.2	4.3
22.3	0.9			547.7	62.1	245.5	27.7	310.7	35.0	165.4	19.0	25.2	2.6
19.2	1.0			449.3	50.8	236.9	26.7	350.6	39.5	89.3	10.7	8.3	0.9
13.8	1.1	239	27	332.6	37.4	227.9	25.7	242.0	27.3	62.9	7.7	4.0	0.5
12.9	1.1	245	28	108.0	12.2	71.3	8.0	52.6	5.9	9.9	1.1	0.3	0.04

Table 4: Measured cross-sections of the ^{nat}Yb(d,x)^{177,175,169}Yb and ^{nat}Yb(d,x)^{173,168,167,165}Tm

Energy E±ΔE (MeV)		Cross section $\sigma \pm \Delta\sigma$ (mb)												
		^{177}Yb		^{175}Yb		^{169}Yb		^{173}Tm		^{168}Tm			^{167}Tm	^{165}Tm
48.2	0.3	2.2	0.3	52.6	6.3	408.9	45.9	1.37	0.24	23.4	2.8	52.8	5.9	10.7	1.4
47.3	0.3	2.3	0.3	55.5	6.6	429.5	48.2	1.63	0.24	18.0	2.4	48.4	5.4	9.5	1.2
45.6	0.4	2.2	0.3	59.2	7.0	429.8	48.3	1.70	0.28	18.5	2.3	39.1	4.4	7.9	1.1
44.7	0.4	2.6	0.3	61.7	7.4	415.9	46.7	1.48	0.30	20.0	2.5	34.1	3.8	5.4	0.8
42.9	0.4	2.3	0.4	68.1	8.0	377.8	42.4	1.93	0.30	17.2	2.2	25.4	2.9	5.0	1.0
42.0	0.4	2.8	0.4	54.9	6.6	358.7	40.3	1.34	0.23	17.5	2.2	21.7	2.5		
40.1	0.5	3.5	0.5	57.4	6.9	310.3	34.9	1.41	0.27	18.9	2.4	13.3	1.5	2.0	0.7
39.1	0.5	3.5	0.4	74.5	8.7	327.2	36.8	1.78	0.28	23.8	3.0	12.4	1.4		
37.2	0.6	3.6	0.5	64.0	7.6	280.5	31.5	1.09	0.21	10.7	1.8	8.5	1.0		
36.1	0.6	4.1	0.6	70.0	8.1	262.5	29.5	1.44	0.23	14.0	2.2	8.0	0.9		
34.1	0.6	4.7	0.6	74.1	8.7	239.6	26.9	2.09	0.33	12.4	1.9	7.7	0.9		
32.9	0.7	4.8	0.6	64.7	7.7	219.9	24.7	1.67	0.29	17.1	2.3	6.4	0.8		
30.7	0.7	5.7	0.7	70.2	8.2	182.4	20.5	1.79	0.30	10.7	1.8	6.9	0.8		
27.9	0.8	6.3	0.8	69.2	8.1	117.0	13.2	1.18	0.20	6.8	1.6	6.5	0.8		
25.2	0.8	8.3	1.0	60.2	7.1	59.7	6.7	0.85	0.16	14.1	1.7	6.1	0.7		
22.3	0.9	9.7	1.1	56.1	6.5	36.8	4.2	0.88	0.15	5.4	1.2	5.7	0.7		
19.2	1.0	12.8	1.5	62.7	7.3	14.5	1.6	0.76	0.17	7.2	1.1				
13.8	1.1	23.5	2.7	62.5	7.3	8.7	0.98	0.63	0.17						
12.9	1.1	25.5	2.9	63.1	7.1	2.7	0.31	0.28	0.04	0.29	0.16				